3-D Turbulent Multiphase Modeling of Molten Steel Flow and Heat Transfer in a Continuous Slab Caster

D.T. Creech and B.G. Thomas,

University of Illinois at Urbana-Champaign, Department of Mechanical and Industrial Engineering, 1206 West Green Street, Urbana, IL USA, 61801

Ph: 217-333-6919; Fax: 217-244-6534

Email: d-creech@uiuc.edu, bgthomas@uiuc.edu

Abstract

A three–dimensional multiphase model of steady turbulent flow and heat transfer in continuous cast steel has been developed using the finite–difference program CFX 4.2. This model was used to evaluate the accuracy of different turbulence models in the difficult task of predicting flow behavior near a wall where there is jet impingement. Liquid steel enters the mold domain through a nozzle. The jet traverses across the cavity to impinge against the far wall. Three turbulence models have been compared: the standard K– ϵ model, the Low Reynolds Number K– ϵ (Low K– ϵ) model at varying grid sizes, and a version of the K– ϵ model with a user supplied wall function for heat transfer. The predicted flow patterns for the standard and user modified K– ϵ models match well with experimental measurements found in the literature. The Low K– ϵ model is very sensitive to grid resolution and only matches experimental flow results at extremely fine grid resolutions. The calculation of heat transfer is more difficult. The standard K– ϵ model greatly under–predicts heat flux and the Low K– ϵ model over–predicts heat flux in the jet impingement zone. Only the K– ϵ model with user supplied wall functions appears capable of matching experimental heat transfer results.

1. Introduction

A schematic of part of the continuous casting process is depicted in Figure 1. Molten steel flows through the "tundish," and then it exits down through a ceramic Submerged Entry Nozzle (SEN) and into the mold. Here, the steel freezes against the water-cooled copper walls to form a solid shell, which is continuously withdrawn from the bottom of the mold at a "casting speed" that matches the flow of the incoming metal. The thickness of the solidifying shell down the mold depends on the amount of heat delivered to it by the nozzle jet. If too much heat is delivered to a point along the shell the jet can melt through the shell, causing the liquid steel to pour out of the caster. This condition is known as a "breakout." If too little heat is delivered to the meniscus area, a frozen "hook" forms, creating a defect in the finished steel. To determine what conditions lead to breakouts and hook defects, we need to accurately predict the heat flux delivered to the shell.

Schematic of continuous casting tundish, SEN, and mold

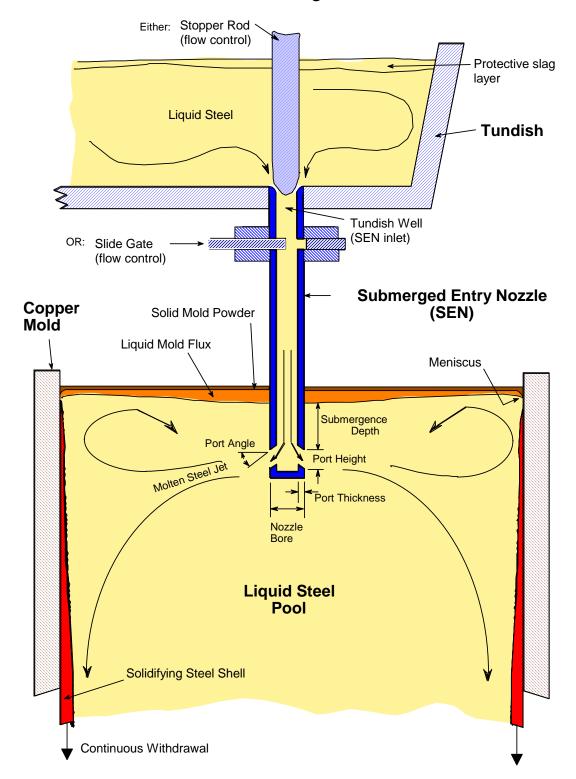


Figure 1. Schematic of tundish and mold region of continuous casting process

The continuous casting process makes heat transfer predictions difficult for several reasons. First, the flow is highly turbulent, and requires the use of turbulence models. Secondly, molten steel has a Prandtl number near 0.1, which is lower than generally used for correlating the standard turbulence model parameters. Finally, the region where the jet impinges on the mold wall dominates heat transfer. This presents a challenge to turbulence models that are derived assuming that flow is parallel to the wall.

2. Turbulence Models

To solve turbulent flows, viscosity is increased in the Navier-Stokes equations, so that relatively course grids can be used, and consequently only large scale turbulent eddies are simulated. There are several turbulence models available in CFX. The most commonly used model is the standard K-ε model. This model uses empirical correlations called wall laws to define the boundary conditions at walls. Alternatively, the Low Reynolds Number K-ε model computes the flow up to the wall. This method requires the use of a grid fine enough to resolve the wall boundary layer.

The heat transfer solution depends on both the corresponding flow solution, which has been calculated previously [1], and the wall boundary conditions. The CFX implementation of the standard K-ε model wall laws, including the wall law for enthalpy, is compared to user-subroutine form of the same equations. The derivation of the wall law implemented in the user subroutine is provided in Appendix A. The user Fortran code, which can be used in the USRWTM subroutine, is provided in Appendix B.

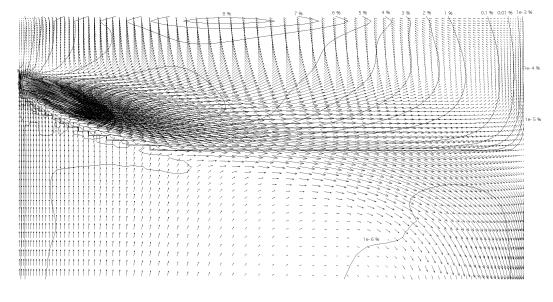
In this study, flow and heat transfer predictions are compared for these different turbulence models. In addition, predictions from several different simulations using the Low K- ϵ model are compared for various grid resolutions. The grid resolutions are expressed in terms of the nondimensional size of the cell near the wall, y^+ , which is defined as

$$y^{+} = \frac{\left(\rho^{2} C_{\mu}^{1/2} K\right)^{1/2}}{\mu} d$$

where d is normal distance from the wall to the first node.

3. Validation

The fluid flow solution was compared to experimental measurements found in the literature [2]. Figure 2a shows multiphase flow results obtained using CFX with the standard K- ϵ turbulence model. The predicted flow pattern matches quite well with the experimental measurements shown in Figure 2b.



a.

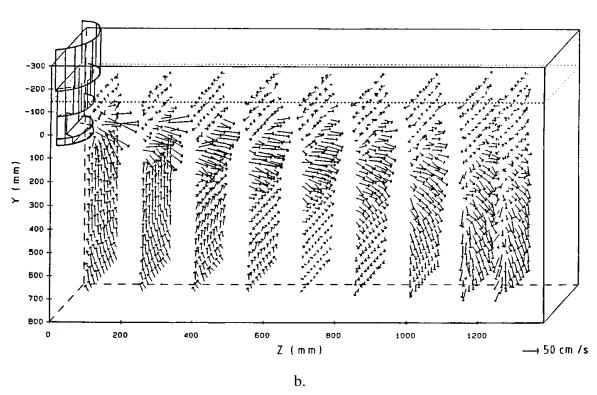


Figure 2. Comparison of velocity profiles in continuous casting mold, a) predicted by current CFX model, and b) measured in a water model [2]

4. Results

Simulations were run for the standard K- ϵ and user modified K- ϵ models with a coarse grid (y⁺=30) and for the Low K- ϵ model with coarse (y⁺<30), fine (y⁺<6) and extremely fine (y⁺<1) grids.

Figure 3 shows profiles of downwards velocity at the solidifying shell on the narrowface wall, 0.741 mm below the steel – flux interface at the top surface of the domain. Each point on the graph represents a grid point, so this figure also illustrates the great differences in mesh refinement between the grids. The dashed line for the standard (high) K- ϵ model illustrates the wall function solution assumed in the model.

This high-speed flow system develops a high velocity gradient near the wall. The standard and Low K- ϵ model with the fine and extremely fine grids predict this high velocity gradient. The Low K- ϵ model with the coarse grid predicts a much lower velocity gradient. Because the Low K- ϵ model does not use wall laws, a fine mesh should be used to resolve the boundary layer. The unrealistic result illustrates the inaccuracy in the flow prediction that can result from using a coarse mesh with the Low K- ϵ model. The standard wall law is able to capture the steep gradient even with the same coarse mesh.

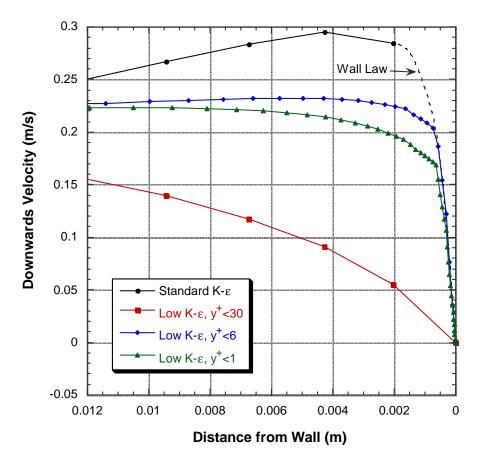


Figure 3. Wall velocity profiles at 0.741 m below the meniscus

The heat transfer prediction is much more sensitive to the turbulence model and grid size than is the flow prediction. Figure 4 shows the centerplane temperature predictions for each turbulence model. The corresponding wall heat flux profiles are shown in Figure 5. The size of the hot area (light shades) shows how much heat is removed from the jet by the walls. The standard K-ε model (a) has the largest hot area, consistent with the prediction that only a small amount of heat is removed by the wall for this model. The User subroutine and Low K-ε models have much smaller hot areas, corresponding with a

larger amount of heat removed by the wall. The course grid Low K-e model (e) has the coldest fluid (largest dark area) and corresponding highest heat flux.

The peak of the heat flux profile occurs at the jet impingement point. The standard K- ϵ model has a very low heat flux peak at this point, while the user modified K- ϵ model has a higher peak. The Low K- ϵ models all have extremely high and narrow peaks. As the grid is refined for the Low K- ϵ model, the heat flux profile becomes narrower.

The total heat removed along the wall is shown in Table 1. The K- ϵ model with user wall law delivers 17% more heat to the wall than the standard K- ϵ model. The Low K- ϵ models with $y^+<30$ and $y^+<6$ grids delivers considerably more heat to the wall than the user-modified K- ϵ model. The heat delivered to the wall by the Low K- ϵ model with $y^+<1$ grid is comparable to the user-modified K- ϵ model.

The heat transfer predictions of the different models were input to a solidification model [3,4] and the predicted shell growth was compared with experimental measurements obtained from a shell obtained from an operating caster [5]. The user-subroutine K- ϵ model prediction matched the experimental data well. The standard K- ϵ model would over-predict shell growth and miss the important shell thinning effect that was observed at the impingement point. The Low K- ϵ model with y⁺<30 would greatly under-predict shell growth.

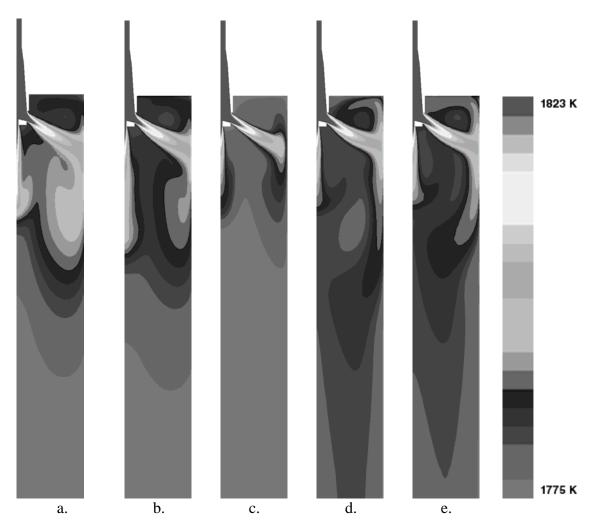


Figure 4. Temperature predictions for a) Standard K-e model, b) User K-e model, c) Low K-e model with $y^+<30$, d) Low K-e model with $y^+<6$ and e) Low K-e model with $y^+<1$ grid.

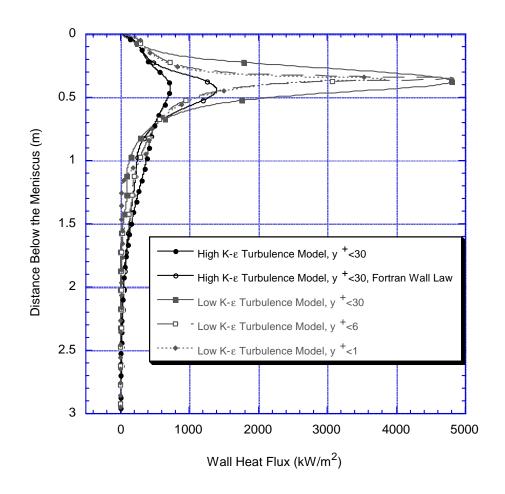


Figure 5. Profiles of wall heat flux at the solidifying shell

Turbulence Model

	` ,
High K-ε Turbulence Model, y ⁺ <30	680.3
High K-ε Turbulence Model, y ⁺ <30, Fortran Wall Law	798.9
Low K-ε Turbulence Model, y ⁺ <30	1490.1
Low K-ε Turbulence Model, y ⁺ <6	996.5
Low K-ε Turbulence Model, y ⁺ <1	901.2

Heat Flux (kW/m)

Table 1. Integrated wall heat flux at the solidifying shell

5. Conclusions

The Low K- ϵ model is very sensitive to grid refinement, and produces unreliable results at coarse grid sizes. The K- ϵ model, as implemented by CFX, produces different results than when the enthalpy wall law is implemented in Fortran subroutines. This suggests that the CFX implementation of the K- ϵ model differs from the textbook definition.

The heat flux predicted by Low K- ϵ model with the $y^+<1$ grid and the user-modified K- ϵ model differ mainly by the shape of the heat flux peak in the impingement region. It is not known which shape is correct, but it is suspected that the user-modified K- ϵ model prediction is better. In real life, the jet moves between several steady flow patterns, spreading out the region where heat is delivered. Thus, the very sharp heat flux peak appears to be unlikely.

Using the Fortran wall law heat transfer results in a solidification model produced shell growth predictions that closely match experimental data [3,4,5]. This suggests that this modeling approach has great potential benefit for predicting, understanding, and avoiding shell-thinning problems such as breakouts.

6. References

- 1. Creech, D.T., MS Thesis, University of Illinois at Urbana-Champaign, in progress.
- 2. Andrzejewski, P.; Kohler, K.-U.; and Pluschkeli, W.; "Model Investigations on the Fluid Flow in Continuous Casting Molds of Wide Dimensions", Steel Research, Vol. 63, No. 6, pp. 242-246, 1992.
- 3. Thomas, B.G., ed., "Mathematical Models of Continuous Casting of Steel Slabs", Annual Report to Continuous Casting Consortium, UIUC, August 21, 1998.
- 4. Stone, D., MS Thesis, University of Illinois at Urbana-Champaign, in progress.
- 5. Thomas, B.G., R.J. O'Malley, and D.T. Stone, "Measurement of temperature, solidification, and microstructure in a continuous cast thin slab", *Modeling of Casting, Welding, and Advanced Solidification Processes VIII*", B.G. Thomas and C. Beckermann, eds., (San Diego, CA, June 7-12, 1998), TMS, Warrendale, PA, 1998, pp. 1185-1199.

Appendix A. Derivation of Wall Law for Heat Transfer

In CFX, we change a wall law with the USRWTM Fortran subroutine by specifying the turbulent multiplier, which is defined as

$$TMULT = \frac{Variable\ at\ Wall-Variable\ at\ Nearest\ Node}{Flux\ of\ Variable}$$

Fourier's Law of heat conduction is

$$q = -\frac{k_t}{C_n} \frac{dH}{dx}$$

where k_t is the turbulent conductivity of the fluid, H is enthalpy, and C_p is the specific heat of the fluid.

For the enthalpy equation, the turbulent multiplier becomes

$$TMULT = \frac{dH}{q} = \frac{k_{t}}{C_{p}dx}$$

The turbulent conductivity is defined as

$$k_{t} = \frac{C_{p} \mu_{t}}{\text{Pr}_{t}}$$

where μ_t is the turbulent viscosity and Pr_t is the turbulent Prandtl number.

The turbulent viscosity is defined as

$$\mu_{t} = \frac{C_{\mu}K^{2}\rho}{\varepsilon}$$

where C_{μ} is the constant 0.09, K is the turbulent kinetic energy, and ε is the turbulent dissipation.

Substituting for μ_t and k_t , the turbulent multiplier can be rewritten as

$$TMULT = \frac{C_{\mu}K^{2}\rho}{\varepsilon \operatorname{Pr}_{c} dx}$$

Appendix B. User Wall Law for Heat Transfer

```
C----TURBULENT WALL LAW TO CORRECT HEAT TRANSFER AT WALLS
07/01/98 DAVID T. CREECH
C**********************
     CALL IPALL('*', 'WALL', 'PATCH', 'CENTRES', IPT, NPT, CWORK, IWORK)
  FIND VARIABLE NUMBER FOR ENTHALPY
 CALL GETVAR('USRWIM','H','IVI
IF ENTHALPY EQUATION SET MULTIPLIER
IF (IVAR.EQ.IEQN) THEN
                                ',IVAR)
     IF (IVAR.EQ.IEQN, IREM
PRANDT = PRT(IVAR,1)

DO 120 I = 1, NPT
   INODE = IPT(I)
   IBDRY = INODE - NCELL
   LCV = IBDRY - ISTART + 1
   INODE1 = IPNODB(IBDRY,1)
        CMU = 0.09

DENS = DEN(INODE1,1)

DENSQK = DEN(INODE1,1) * SQRT( TE(INODE1,1) )
        EPSILON = ED(INODE, 1)
        AKE = TE(INODE1,1)
AKK = AKE*AKE
    CALCULATE NORMAL DISTANCE FROM NODE TO WALL
С
        DN = YWALL(LCV)
С
         WRITE(NWRITE, *) YWALL(LCV)
C
C
     COMPUTE MULTIPLIER
        TMULT(LCV,1) = (CMU*DENS*AKK)/(PRANDT*DN*EPSILON)
 120 CONTINUE
     END IF
```